

**Universal long-time behavior of aperiodically driven interacting quantum systems**

Zi Cai

*Department of Physics and Astronomy, Shanghai Jiao Tong University, Shanghai 200240, People's Republic of China  
and Institute for Quantum Optics and Quantum Information, Austrian Academy of Sciences, 6020 Innsbruck, Austria*

Claudius Hubig and Ulrich Schollwöck

*Department of Physics and Arnold Sommerfeld Center for Theoretical Physics, Ludwig-Maximilians-Universität München,  
Theresienstraße 37, 80333 Munich, Germany*

(Received 4 April 2017; published 9 August 2017)

Understanding the collective dynamics in many-particle systems is of important significance in nonequilibrium physics. In this paper, we systematically study the long-time behavior in stochastically driven interacting quantum systems. We find that even though the stochastic forces will inevitably drive a system into a featureless steady state, the asymptotic behavior to approach the steady state can be highly nontrivial and exhibits rich universal dynamics due to the interplay between the stochastic driving and quantum many-body effects. Special attention is devoted to the effect of the mode-coupling perturbations, which may have important consequence for the long-time dynamics of the stochastically driven quantum many-body systems.

DOI: [10.1103/PhysRevB.96.054303](https://doi.org/10.1103/PhysRevB.96.054303)**I. INTRODUCTION**

Recently, nonequilibrium quantum many-body physics has attracted considerable attention due to enormous progress in ultracold atomic experiments [1], in which interacting quantum systems can be driven out of thermodynamic equilibrium by quenching [2–6], ramping [7], and periodic driving [8–10] of Hamiltonian parameters, or by coupling the systems to engineered [11–15] or thermal [16–22] baths and external noise [23–30]. A complete understanding of the nonequilibrium systems is an essential theoretical challenge, while incorporating quantum many-body effects further complicates the situation and gives rise to important novel phenomena; e.g., a system subject to external driving forces can display unexpected dynamical and steady properties absent in the nondriven counterpart [31–39]. Up to now, most of the research on driven quantum many-body systems has been devoted to the periodically driven cases [40–46], while their stochastic counterpart is much less studied. In spite of the fact that stochastic driving of a quantum system will inevitably lead to decoherence and heat the system towards an infinite-temperature state, the way to approach this featureless steady state can be highly nontrivial and the interplay between the quantum many-body effect and stochastic driving may give rise to rich dynamical behavior. Moreover, understanding stochastically driven quantum (many-body) systems is not only of high theoretical interest, but also of immense practical significance due to the possible relations to the decoherence problem in quantum simulation and information processing [47].

Among the topics of great current interest in nonequilibrium physics are the abnormal (nonexponential) relaxation dynamics of a perturbed system: in certain types of many-particle systems, the relaxation time can diverge and the resulting power-law abnormal relaxation dynamics can be understood as a collective behavior of independent system modes, each of which decays with its own rate and at least for one mode the relaxation rate vanishes. The situation is significantly complicated in the presence of mode-coupling perturbations

(e.g., interactions), and understanding the complex relaxation dynamics of interacting many-particle systems is of immense significance in rapidly developing interdisciplinary fields between physics, biology, and the social-economical sciences. Even though this problem has been intensively studied by analytic (e.g., renormalization group analysis) and numerical methods based on microscopic master equations or mesoscopic Langevin-type representations in classical physics, our understanding of the abnormal relaxation behavior in quantum many-particle systems is still far from complete.

In this paper, we study the abnormal relaxation dynamics of stochastically driven quantum many-body systems. Without loss of generality, we choose one of the simplest stochastic driving protocols: a telegraph-like driving where one of the Hamiltonian parameters randomly jumps between two discrete values during the time evolution. This type of noise has recently been introduced in condensed matter physics to model the noise effect on the intensively studied Majorana fermions [47]. As we will show in the following, the results derived from this specific example can also apply for more general stochastic driving protocols. The goal in this paper is to understand the statistical long-time behavior of many-body quantum systems driven by a stochastic sequence of sudden quenches (see Fig. 1), and its dependence on the specific form of the Hamiltonian and various perturbations, especially the interactions. In general, the Hamiltonian of quantum lattice systems can be classified into two categories according to its local Hilbert space being bounded or not, whose long-time heating dynamics are fundamentally different from each other (e.g., a system with unbounded local Hilbert space can absorb energy indefinitely and thus the steady state is ill defined). To provide a comprehensive understanding of the stochastically driven interacting quantum systems, we study two representative examples of quantum many-body Hamiltonians: a one-dimensional (1D) spinless fermionic model and a two-dimensional (2D) bosonic quantum  $O(N)$  model (see Fig. 1), representing the Hamiltonian with locally bounded and unbounded Hilbert space, respectively. By exploring the long-time behavior in these concrete models, we have taken

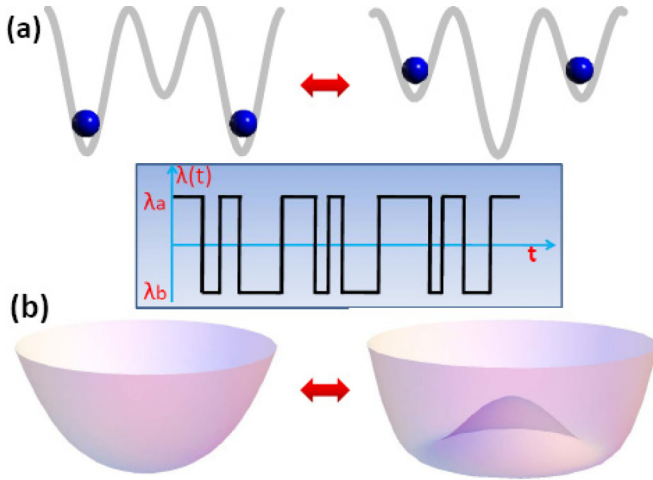


FIG. 1. Sketches of the two models studied in this paper. (a) A 1D spinless fermion model with fluctuating staggered potential and (b) a 2D quantum  $O(N)$  model with a fluctuating mass. The inset is an example of a typical trajectory of the telegraph-like stochastic driving parameter  $\lambda(t)$ .

a first step towards understanding the stochastically driven interacting quantum systems.

The paper is organized as follows: In Sec. II, we propose a general method to deal with the quantum many-body systems with telegraph-like stochastic driving, and discuss its limitations. In Sec. III, we study a 1D spinless fermionic model with a stochastically fluctuating staggered potential, which exhibits algebraic relaxation dynamics. This algebraic long-time behavior is then investigated in the broader context of a more general system Hamiltonian (gapped or gapless) and driving protocols (multicolored), and we provide general criteria for its existence. We further examine the effect of two typical mode-coupling perturbations—disorder and interaction—and find that both of them have important consequence for the long-time dynamics of the system. In Sec. IV, we study a 2D quantum  $O(N)$  model with a fluctuating mass that drives the system crossing the phase boundary of the equilibrium phase diagram. At least in the large- $N$  limit, we find that the interaction will significantly suppress the heating dynamics and change the divergent behavior from exponential to algebraic. Sections V and VI contain a discussion of possible experimental realizations and an outlook.

## II. MARGINAL DENSITY MATRIX METHOD

In this paper, we consider stochastically driven quantum many-body systems in which one parameter  $\lambda(t)$  in the Hamiltonian randomly jumps between two values  $\lambda_a$  and  $\lambda_b$  with a transition rate  $\kappa$  during time evolution. For a given trajectory of the parameter  $\{\lambda(t)\}$  (e.g., the inset of Fig. 1), the system evolves unitarily with a time-dependent Hamiltonian and can be described by the density matrix  $\rho_{\{\lambda(t)\}}(t)$ . Since we are interested in the statistical long-time behavior of this stochastically driven system near the steady state (infinite-temperature state), we perform the ensemble averages over all the stochastic trajectories. Our goal is to derive an equation of motion (EOM) for the average density

matrix  $\rho_s(t) = \langle \rho_{\{\lambda(t)\}}(t) \rangle_s$  where the angular brackets  $\langle \cdot \rangle_s$  denote the ensemble average over all stochastic trajectories. To achieve this goal, we introduce the marginal density matrix  $\rho_{a(b)}(t)$  in which the ensemble average is over those trajectories satisfying  $\lambda(t) = \lambda_{a(b)}$ :

$$\rho_{a(b)}(t) = \langle \rho(t) \delta(\lambda(t) - \lambda_{a(b)}) \rangle_s. \quad (1)$$

Obviously  $\rho_s(t) = \rho_a(t) + \rho_b(t)$ . The average of physical observables is defined as  $\langle \hat{O} \rangle = \text{Tr}(\hat{O} \rho_a) + \text{Tr}(\hat{O} \rho_b)$ . The marginal density matrix method was first introduced by Zoller *et al.* in the context of quantum optics [48] and has recently been introduced in condensed matter physics [47]. We can prove (see Appendix A and Ref. [47]) that the EOM of the marginal density matrix is described by the following master equation:

$$\begin{aligned} \frac{d\rho_a(t)}{dt} &= i[\rho_a, \hat{H}_a] - \kappa\rho_a + \kappa\rho_b, \\ \frac{d\rho_b(t)}{dt} &= i[\rho_b, \hat{H}_b] + \kappa\rho_a - \kappa\rho_b, \end{aligned} \quad (2)$$

where  $\hat{H}_{a(b)}$  is the time-independent Hamiltonian for  $\lambda(t) = \lambda_{a(b)}$ , and  $\kappa$  is the transition rate. Assuming the dimension of the Hilbert space of the system is  $N$ , we can rewrite the  $N \times N$  density matrix  $\rho_{a(b)}$  into an  $N^2$ -dimensional vector  $\vec{\rho}_{a(b)}$ , and the master equation Eq. (2) turns to

$$\frac{d\vec{\rho}_s}{dt} = \hat{\mathbb{L}} \vec{\rho}_s \quad (3)$$

in which  $\vec{\rho}_s = [\vec{\rho}_a, \vec{\rho}_b]^T$  is a  $2N^2$ -dimensional vector and  $\hat{\mathbb{L}}$  is the  $2N^2 \times 2N^2$  Liouville superoperator defined in Eq. (2). For a quadratic Hamiltonian with translational symmetry, we can perform a Fourier transformation  $H_{a(b)} = \sum_k H_k^{a(b)}$ , and the Liouville superoperator can be decomposed as  $\hat{\mathbb{L}} = \bigoplus_k \mathbb{L}_k$ . In general, the long-time behavior of the system is determined by the spectrum (eigenvalues) of  $\mathbb{L}_k$ . From Eq. (2), we can find that the steady state is always a unit matrix irrespective of the specific form of the Hamiltonian:  $\rho_a^s = \rho_b^s = \hat{\mathbb{1}}/(2N)$ , corresponding to the infinite-temperature state. The above method can be straightforwardly generalized to a more general driving protocol with the controlling parameter fluctuating between  $\mathcal{N}$  discrete values, where the marginal density matrix  $\vec{\rho}_s = [\vec{\rho}_1, \dots, \vec{\rho}_{\mathcal{N}}]^T$ .

Before we proceed further to discuss specific examples, we make some remarks about the method. Compared to the conventional method of calculating unitary evolution for each given trajectory and then doing the ensemble average, the marginal density matrix method has the advantage of the absence of stochasticity. The ensemble average has already been performed implicitly in Eq. (2) with the price of the Hilbert space being significantly enlarged from  $N$  to  $2N^2$ . For a fermionic or bosonic quadratic Hamiltonian, the EOM of the system can be reduced to that of the single-particle correlation functions taking advantage of Wick's theorem; thus the dimension of the reduced EOM is proportional to the system size  $L$ . However, for a genuine interacting quantum many-body system  $N \sim O(e^L)$ ; thus it is not convenient to directly solve Eq. (2) for large systems.

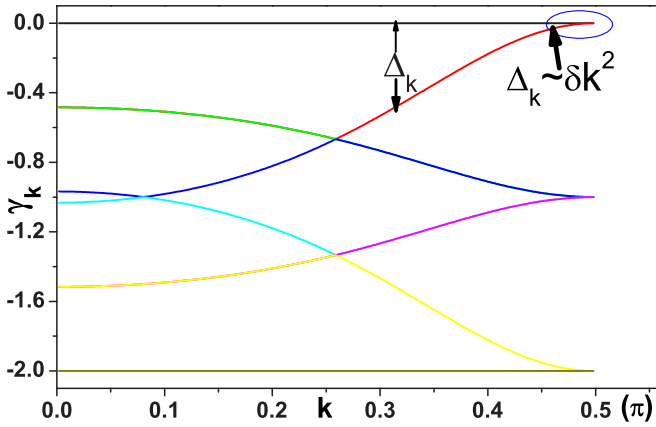


FIG. 2. The spectrum of the (noninteracting) Liouville superoperator  $\mathbb{L}_k$  with parameters  $\delta = J, \kappa = J$ .

### III. ONE-DIMENSIONAL SPINLESS FERMION

#### A. Algebraic long-time dynamics: A collective behavior of independent momentum modes

The first model we consider is a 1D spinless fermionic model with a stochastically fluctuating staggered potential with the Hamiltonian  $H = H_0 + H'$ , where  $H_0$  is the Hamiltonian of the noninteracting fermions with stochastic driving:

$$H_0 = \sum_{i,\sigma} -J(c_i^\dagger c_{i+1} + \text{H.c.}) - \sum_i \lambda(t)(-1)^i n_i. \quad (4)$$

$c_i^\dagger (c_i)$  is the creation (annihilation) operator of the spinless fermion and  $n_i = c_i^\dagger c_i$  is the local density operator.  $\lambda(t)$  stochastically jumps between  $\lambda_a = \delta$  and  $\lambda_b = -\delta$  with jump rate  $\kappa$ .  $H'$  represents different kinds of perturbations that will be explicitly analyzed below. We assume that initially the system is in the ground state of  $H_a$ , and focus on the population imbalance  $P(t) = \sum_i (-1)^i n_i / L$  ( $L$  is the number of lattice sites). As we analyzed above, the infinite- $T$  state always plays the role of an attractor during the time evolution, and we will explore the relaxation dynamics towards this fixed point.

We first consider the unperturbed case ( $H' = 0$ ), where the translationally invariant system without interaction is best treated in a Fourier-transformed picture as a collection of independent momentum ( $k$ ) modes ( $-\pi/2 < k < \pi/2$ ; we take the lattice constant to be 1). In the long-time limit, each  $k$  mode will decay exponentially with time  $\sim e^{-\Delta_k t}$ , where  $\Delta_k$  is the gap of  $\mathbb{L}_k$  (the absolute value of the second largest real part of the eigenvalues of  $\mathbb{L}_k$ ), which vanishes at  $k_c = \pi/2$ , and can be expanded around  $k_c$  as  $\Delta_k = \alpha(\delta k)^2$  with  $\delta k = k - k_c$  (the first order of  $\delta k$  vanishes for symmetry reason), as shown in Fig. 2. The dynamics of physical observables results from the collective behavior of all  $k$  modes, and the long-time asymptotic behavior is determined by the long-lived modes ( $k$  modes near the gapless point):

$$P(t) \sim \int_0^\infty d\delta k e^{-\alpha\delta k^2 t} \sim t^{-1/2}. \quad (5)$$

This agrees with our numerical results shown in Fig. 3(a), that the long-time behavior of  $P(t)$  always decays algebraically

with time:  $P(t) \sim t^{-\eta}$ , with a universal exponent  $\eta = 1/2$  independent of the system parameters.

In the following, we will investigate this algebraic relaxation dynamics in a broader context to demonstrate that it is not an artifact of a specific Hamiltonian with a peculiar driving protocol. We first examine a more general driving protocol where  $\lambda(t)$  is randomly fluctuating between  $\mathcal{N}$  discrete values:  $\lambda_i = \lambda - (i-1)\Delta\lambda$  with  $i = 1, \dots, \mathcal{N}$  and  $\Delta\lambda = 2\lambda/(\mathcal{N}-1)$ . Without loss of generality, we assume that the jump process can only occur between adjacent values of  $\{\lambda_i\}$  (e.g.,  $\lambda_i \rightarrow \lambda_{i+1}$  or  $\lambda_{i-1}$ ) with a transition rate  $\kappa/2$ . In the limit of  $\mathcal{N} \rightarrow \infty$ ,  $\lambda(t)$  can take any continuous value in the region  $[-\lambda, \lambda]$  during its random-walk dynamics, which represents a typical colorful noise. From Fig. 3(b), we find that the long-time behavior is qualitatively the same as that in the telegraph noise. Second, we keep the telegraph driving protocols but change the system Hamiltonian. It is well known that the ground state and low-energy excited state properties of a gapped and gapless Hamiltonian are significantly different from each other; it is interesting to ask whether the Hamiltonian gap has an important consequence for the long-time dynamics of the stochastically driven system. To examine the role of the Hamiltonian gap, we choose a 1D Kitaev chain as our system Hamiltonian:

$$H_0 = \sum_i (-Jc_i^\dagger c_{i+1} - \Delta c_i^\dagger c_{i+1}^\dagger + \text{H.c.}) - \sum_i \mu n_i + H(t), \quad (6)$$

where  $H(t) = \sum_i \lambda(t)(-1)^i n_i$  represents the same stochastic driving protocol. For simplicity in the following discussion, we choose the pairing term with the same amplitude with the hopping:  $\Delta = J$  in Eq. (6). Without the external driving, this model exhibits two gapped (topological and nontopological) phases in the ground state separated by a gapless critical point at  $\mu = 2J$ . As shown in Fig. 3(c), the Hamiltonian gap does not have important consequence on the long-time relaxation dynamics, which always decay algebraically no matter whether the system is in the topological trivial/nontrivial phases or at the critical point. This result also holds for a different driving protocol with  $H(t) = \sum_i \lambda(t)n_i$ .

Since the algebraic long-time dynamics is so common in stochastically driven quantum (noninteracting) many-body systems, irrespective of the specific driving protocols and the gap/gapless feature of the system Hamiltonian, it is interesting to explore the physics behind it and its universality. Physically, this algebraic decay can be understood as a collective behavior of independent  $k$  modes, and at least one of them is immune to the stochastic driving and thus its relaxation rate vanishes. Mathematically, this universality is related to the absence of a gap in the spectrum of  $\mathbb{L}$  as well as the continuity of  $\Delta_k$  around the gapless point. It is a highly nontrivial question to determine whether a general Liouville superoperator as defined in Eq. (3) is gapped or gapless; there is no general answer. However, for a fermionic system with a quadratic Hamiltonian, we can propose a sufficient condition for the existence of a gapless Liouville superoperator. We take the translationally invariant system as an example, and the results can be easily generalized to other quadratic Hamiltonians. For a translationally invariant system, the Hamiltonian can be decoupled into an independent

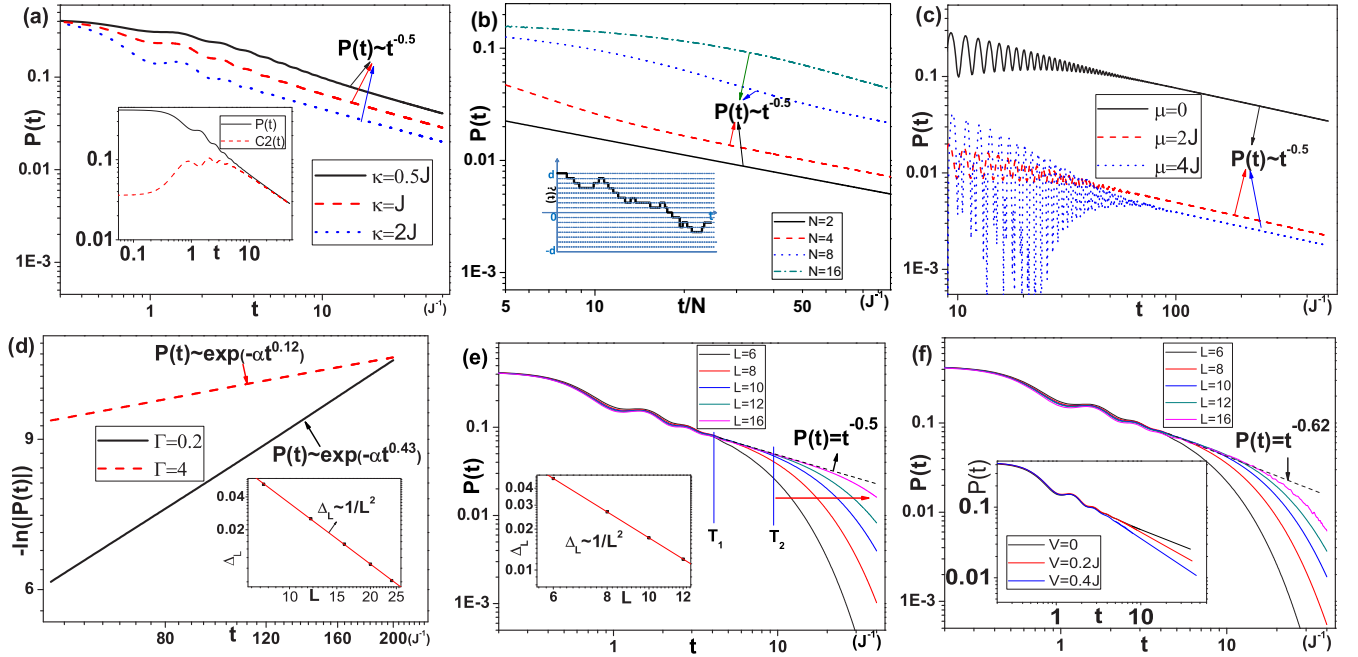


FIG. 3. (a) Time evolution of  $P(t)$  for the noninteracting case with  $\delta = 2J$  and different  $\kappa$  (the inset is the dynamics of both the diagonal and off-diagonal correlation functions). (b) Dynamics of  $P(t)$  with a  $\mathcal{N}$ -state random walk driving protocols. (c) Time evolution for the Kitaev chain model with stochastic driving in different phases with parameters  $\delta = 0.5J$ ,  $\kappa = 2J$  and the perfect CDW state as the initial state. (d) Static disorder [the inset is the finite-size scaling of the Liouville gap  $\Delta_L$  for the noninteracting case, which is obtained by fitting the long-time behavior using the exponential function  $P(t) \sim e^{-\Delta_L t}$ ]. Finite-size effect on the dynamics of  $P(t)$  for (e) the noninteracting case (the inset is the finite-size scaling of  $\Delta_L$  in the presence of strong interaction  $V = 2J$ ) and (f) the weak-interacting case ( $V = 0.2J$ ) (the inset is the extrapolated results for the dynamics in the thermodynamics limit with weak interactions). In both cases open boundary conditions are chosen and the dashed lines are the extrapolated results for the dynamics in thermodynamic limit. For (b) and (d)–(f), we choose the parameters  $\delta = 2J$ ,  $\kappa = 2J$ .

$k$  mode:  $H = \sum_k \mathbf{C}_k^\dagger \hat{H}(k) \mathbf{C}_k$ , in which the Hamiltonian of each  $k$  mode  $\hat{H}_k$  can be decomposed into two parts  $\hat{H}(k) = \hat{H}_1(k) + \lambda(t)\hat{H}_2(k)$  with  $\hat{H}_1(k)$  corresponding to the nondriven part of the Hamiltonian, and  $\lambda(t)\hat{H}_2(k)$  corresponding to the external driving which can be telegraph or of other types. If there exists a  $k$  mode at  $k = k_c$  satisfying  $[\hat{H}_1(k_c), \hat{H}_2(k_c)] = 0$ , then the eigenstates of  $\hat{H}_1(k_c)$  will be immune to the external driving; in other words, at least one nontrivial steady state other than the infinite-temperature one exists at  $k_c$  and this degeneracy and the analyticity of  $\Delta_k$  around  $k_c$  guarantee that the gap of the Liouville superoperator closes at  $k = k_c$ . In the spinless fermion case,  $\hat{H}_1(k_c = \pi/2) = \mathbf{0}$  thus satisfies the conditions. Finally, it is natural to ask whether it is possible to find a long-time behavior different from this algebraic scenario. In Appendix C, we propose a spinful fermion model, which exhibits a dynamical phase transition from an algebraic to exponential long-time relaxation behavior by tuning the Hamiltonian parameters.

### B. Effect of mode-coupling perturbations

As analyzed above, the algebraic long-time dynamics in the stochastically driven quantum many-body system is a collective behavior of independent  $k$  modes. One of the most important questions is how robust the behavior is against perturbations, especially those terms inducing coupling between different modes. In the presence of the mode-coupling perturbations, each mode no longer evolves independently

and the genuine many-body effect can significantly change the long-time behavior and give rise to interesting relaxation dynamics. In the context of nonequilibrium physics of quantum quenches, this problem has been analyzed with the Keldysh technique and renormalization analysis [49,50], and it has been discovered that even those mode-coupling terms irrelevant in equilibrium can have significant consequence on the steady state and the long-time relaxation dynamics. Understanding the effect of the mode-coupling perturbation on the long-time dynamics of stochastically driven quantum many-body systems is the main purpose of this paper.

In classic physics, these nonequilibrium dynamics of interacting many-particle systems have been intensively studied using the Boltzmann equations. In some special situations (e.g., near the phase transition point [51–53]), the renormalization group analysis provides a useful method in determining whether a perturbation is relevant or not for the long-time dynamics. However, due to the intrinsic difficulty of the strongly correlated quantum physics, there is no universal method to study their long-time dynamics. In certain quantum many-body systems with strong decoherence, the off-diagonal terms of the density matrix nearly vanish after long-time evolution, and the dynamics near the steady state could be reduced to effective classic rate equations of the diagonal density matrix elements [25,26]. This quasiclassic approximation, as we will illustrate in the following, does not apply for our cases, where we can find that off-diagonal terms of the density matrix are not neglectable and that the dynamics of the systems are

essentially quantum instead of classic even near the steady state.

In the following, we study two typical mode-coupling mechanisms: disorder and interaction. In the presence of static disorder, the translational invariance is broken and a particle initially in one  $k$  mode can be scattered into another, which corresponds to a first-order mode-coupling mechanism, while in an interacting system, the two-particle scattering process introduces a second-order mode-coupling mechanism with momentum and energy conservations.

*Effect of static disorder.* Now we study the effect of static disorder on the long-time behavior of this stochastically driven system;  $H' = \sum_i V_i n_i$ , where  $V_i$  represents static disorder sampled from a uniform random distribution with  $V_i \in [-\Gamma, \Gamma]$ . From Fig. 3(d), we find that even weak disorder ( $\Gamma \ll J$ ) will qualitatively change the long-time behavior of the system from an algebraic decay to a stretched exponential decay:

$$P(t) \sim \exp(-\alpha t^\beta), \quad (7)$$

where  $0 < \beta < 1$  is a nonuniversal parameter which depends on the parameters in the Hamiltonian. These unconventional relaxation dynamics were first discovered in 1847 by Kohlrausch, and have been observed in various systems such as molecular [54] and spin [55] glasses and dissipative interacting quantum systems [56–60]. Up to now, considerable theoretical effort has been devoted to understanding the origin of the stretched exponential decay [61–63]. For the system considered above, we can propose a simple understanding of the unconventional relaxation dynamics by considering an extreme situation, where  $V_i$  can only take two discrete values 0 and  $\infty$  with the probability  $p$  and  $1 - p$  ( $0 < p < 1$ ). In this case, the system turns to a site-diluted model composed of open chains (clusters) with different lengths. Notice that for a cluster with length  $l$ , its relaxation time  $\tau_l \sim l^2$  [as shown in the inset of Fig. 3(d)]; therefore the long clusters dominate the long-time dynamics of the system. On the other hand, in a site-diluted chain, the appearance of the long clusters is a rare event with a probability exponentially decaying with length  $l$ :  $W_l = p^l = e^{(\ln p)l}$ . Under these approximations, the long-time behavior of the system can be obtained as  $P(t) \sim \int dl W_l l e^{-t/\tau_l} = \int dl l e^{-(c'l + \frac{t}{l^2})}$ , where  $c' = -\ln p$ . For large  $t$ , this integral can be evaluated in the saddle-point approximation, and we obtain  $P(t) \sim \exp[-\tilde{c}t^{\frac{1}{3}}]$ .

*Effect of interaction.* In all the cases studied previously, the Hamiltonians are of quadratic form. Hence, the information on the system can be obtained from the single-particle correlation functions. To investigate the dynamics of a genuine interacting quantum many-body system, we consider the perturbation  $H' = \sum_i V n_i n_{i+1}$  representing nearest-neighbor (NN) interactions between the spinless fermions. As pointed out previously, for this interacting case, the dimension of the EOM in Eq. (2) grows fast with the system size  $2N^2 \sim O(e^{2L})$ . This makes it impractical for large systems. An alternative method is to calculate the unitary evolution for each given stochastic trajectory and then explicitly perform the ensemble average over a sufficiently large number of trajectories. The dimension of the EOM in the unitary evolution method (UEM)  $N \sim O(e^L)$ , even though much smaller than that in the

marginal density matrix method (MDMM), is still exponential in lattice site. To extrapolate the long-time behavior of an interacting quantum system in the thermodynamic limit based on the finite-size results, we need to carefully study the role of finite-size effects.

To gain some insight into the finite-size effects, we first focus on the noninteracting case. From Fig. 3(e) we find that for a finite-size system the time evolution can be divided into three regimes by two time scales  $T_1$  and  $T_2$ : the short-term dynamics ( $t < T_1$ ) is characterized by the coherence oscillations and depends on the initial state; once the initial state information is lost, the systems enter the intermediate regime ( $T_1 < t < T_2$ ) exhibiting a power-law behavior. Since any finite system has a nonzero Liouville gap, the finite-size effect will dominate the long-term evolution ( $t > T_2$ ) and lead to an exponential decay with time. From Fig. 3(e) we find that the time scale  $T_1$  is insensitive to the system size  $L$ , while  $T_2$  monotonically increases with  $L$ . Therefore, we expect that in the thermodynamic limit  $L \rightarrow \infty$ , the long-term exponential dynamics will give way to the intermediate algebraic dynamics, which represents the long-time behavior of the system. This tendency can be seen clearly even for small systems ( $L \leq 16$ ).

For interacting systems, we expect that the above dynamical structure of the time evolution still holds at least for weak interactions  $V \ll J$ , which allows us to extract the long-time behavior from the intermediate dynamics of finite-size systems. The dynamics of  $P(t)$  in the presence of a weak interaction is shown in Fig. 3(f), where we find that the structure of the dynamic behavior is similar to that of the noninteracting case. However, the exponent of the power-law decay in the intermediate region is changed by the interaction to  $P(t) \sim t^{-\beta}$  with  $\beta > 0.5$ , which reminds us of the algebraic correlation functions in the Luttinger liquid whose power-law exponents are also renormalized by interaction [64]. Recently, similar anomalous power law dynamics have also been observed in the many-body localization systems [65]. The finite-size scaling indicates that, similarly to the noninteracting case, this intermediate algebraic regime with a renormalized exponent can also be extrapolated to infinite time in the thermodynamic limit. A physical picture is that the interaction makes the momentum modes no longer independent of each other, and the scattering between them leads to transitions between the fast and slow modes, and thus makes the decay faster than that in the noninteracting case. Recently, a similar dynamical behavior has been observed in the relaxation dynamics of many-body localized systems [66,67]. For strong interactions, the dynamical structure is complex and does not resemble the noninteracting case; thus to extract the long-time behavior requires larger systems, which is beyond the capability of the current method. The only information we can obtain about the strongly interacting case is that the finite-size scaling [inset of Fig. 3(e)] indicates that the Liouville gap vanishes in the thermodynamic limit as  $\Delta_L \propto 1/L^2$ , which precludes the possibility of exponential decay for  $L \rightarrow \infty$  in the long-time behavior.

### C. Discussion

At the end of this section, we add some remarks. First, we shall compare our results of the stochastically driven systems

with those in their periodical counterparts, where the periodic driving may either drive the system to time-periodic regimes synchronous [40] or asynchronous [43] with the driving, or heat the system to an infinite-temperature state [41] after an extraordinarily long time, and the asymptotic dynamics depend on many details of the systems [40–44]. For the stochastic cases, the external driving will heat and drive the system into the “long-time” asymptotic regime after a relatively short time  $T_1 \sim O(J^{-1})$ . Due to the ensemble average, the stochastic driving facilitates the stabilization of the system into a universal dynamical regime, which enables us to study the dynamical universality. Second, since stochastic driving causes decoherence, one might expect that the off-diagonal terms of the density matrix vanish after long-time evolution, and all the previously studied dynamics near the steady state could be reduced to a classic rate equation of the diagonal matrix elements. Thus, the dynamics would be essentially classic. To clarify this point, we calculate the dynamics of one of the off-site correlations  $C_2(t) = \langle c_i^\dagger c_{i+2} \rangle$  as a representative of the off-diagonal elements of the density matrix, and compare it to that of the typical diagonal one  $P(t)$ . As shown in the inset of Fig. 3(b),  $C_2(t) \sim t^{-0.5}$  decays as slowly as  $P(t)$ , which indicates that even near the infinite-temperature state, the quantum fluctuations still play an important role and the dynamics are not classical.

#### IV. QUANTUM $O(N)$ MODEL IN THE LARGE- $N$ LIMIT

In the last section, we studied an example with a locally bounded Hilbert space, where the infinite temperature state is well defined (the unit matrix in the Hilbert space) and all physical observables will converge eventually. However, for systems with a locally unbounded Hilbert space, the stochastic driving force can infinitely heat the systems and the physical observables will diverge with time. Hence, we expect that the long-time behavior will be fundamentally different from the previously studied cases. As an example, we consider a quantum  $O(N)$  model in the large- $N$  limit, which provides a paradigm to understand symmetry breaking in statistical mechanics, and both its equilibrium properties and unitary dynamics can be solved exactly in different dimensions. More precisely, we study a 2D quantum  $O(N)$  model with a fluctuating mass that drives the system across the phase boundary of the equilibrium phase diagram. Taking the advantage of infinite  $N$ , the Hamiltonian of the interacting quantum system can be reduced to a quadratic form with a time-dependent parameter that is self-consistently determined during the time evolution, which allows us to study the dynamics of these genuine interacting quantum many-body systems, e.g., the quantum quench [68] and periodically driven [43] problems.

The Hamiltonian of a quantum  $O(N)$  model with a fluctuating mass reads

$$H = \int d^d \mathbf{x} \frac{|\vec{\pi}(\mathbf{x})|^2}{2} + \frac{|\nabla \vec{\phi}(\mathbf{x})|^2}{2} + \frac{r(t)}{2} |\vec{\phi}(\mathbf{x})|^2 + \frac{U}{4N} [|\vec{\phi}(\mathbf{x})|^2]^2, \quad (8)$$

where  $\vec{\phi}(\mathbf{x}) = [\phi_1(\mathbf{x}), \dots, \phi_N(\mathbf{x})]$  are  $N$ -component real vector field operators and  $|\vec{\phi}(\mathbf{x})|^2 = \sum_i \phi_i^2(\mathbf{x})$ .  $\vec{\pi}(\mathbf{x})$  are conjugate field operators of  $\vec{\phi}(\mathbf{x})$  that satisfy the commutation relation  $[\phi_i(\mathbf{x}), \pi_j(\mathbf{x}')] = \delta_{ij} \delta(\mathbf{x} - \mathbf{x}')$ .  $r(t)$  is a time-dependent mass term. It randomly jumps between two values  $r_a$  and  $r_b$  with the transition rate  $\kappa$ . For  $d \geq 2$ , the equilibrium critical point between ferromagnetic and paramagnetic phases is identified by the condition  $r_c = -\frac{U}{4} \int_k \frac{1}{k^2}$  (from now on we define  $\int_k = \int^\Lambda \frac{d^d \mathbf{k}}{(2\pi)^d}$  with  $\Lambda$  the ultraviolet cutoff in momentum space).

*Paramagnetic case.* We first discuss the case where the initial state is prepared in the paramagnetic region, where the  $O(N)$  symmetry is preserved during the time evolution. The interaction terms can be decoupled by introducing the auxiliary field  $\rho(\mathbf{x}, t)$  as

$$e^{-\frac{U}{4N} [|\vec{\phi}(\mathbf{x})|^2]^2} = \int \mathcal{D}[\rho] e^{-i\frac{U}{2} \rho(\mathbf{x}, t) |\vec{\phi}(\mathbf{x})|^2 - \frac{UN}{4} \rho^2(\mathbf{x}, t)}. \quad (9)$$

For  $N \rightarrow \infty$ , the fluctuations are suppressed by the large- $N$  effect, and the auxiliary field  $\rho(\mathbf{x}, t)$  can be replaced by its saddle point value  $\rho(\mathbf{x}, t) = -if(t)$  with  $f(t) = \int d^d \mathbf{x} (|\vec{\phi}(\mathbf{x})|^2) / N$  [69]. Performing the Fourier transformation  $\phi_i(\mathbf{x}) = \int_k e^{i\mathbf{k}\cdot\mathbf{x}} \phi_i(\mathbf{k})$  and introducing the ladder operators  $a$  and  $a^\dagger$  [70] by  $\phi(\mathbf{k}) = \frac{1}{\sqrt{2}}(a_{\mathbf{k}} + a_{-\mathbf{k}}^\dagger)$ ,  $\pi(\mathbf{k}) = \frac{i}{\sqrt{2}}(a_{-\mathbf{k}}^\dagger - a_{\mathbf{k}})$ , where  $[a_{\mathbf{k}}, a_{\mathbf{k}'}^\dagger] = (2\pi)^d \delta(\mathbf{k} - \mathbf{k}')$ , the Hamiltonian turns into

$$H = \int_k \frac{1 + \delta}{2} (a_{\mathbf{k}}^\dagger a_{\mathbf{k}} + a_{-\mathbf{k}} a_{-\mathbf{k}}^\dagger) + \frac{\delta}{4} (a_{\mathbf{k}}^\dagger a_{-\mathbf{k}}^\dagger + a_{-\mathbf{k}} a_{\mathbf{k}}), \quad (10)$$

where  $\delta = r(t) + k^2 + Uf(t) - 1$ . In the following, we will focus on the self-consistent field  $f(t) = \int_k f_{\mathbf{k}}(t)$  where  $f_{\mathbf{k}}(t) = \langle \phi(\mathbf{k}) \phi(-\mathbf{k}) \rangle$ . To study the time evolution of  $f(t)$ , we introduce the vector representation of the bosonic correlation functions  $\vec{G}_{\mathbf{k}} = [ \langle a_{\mathbf{k}}^\dagger a_{\mathbf{k}} \rangle, \langle a_{\mathbf{k}}^\dagger a_{-\mathbf{k}}^\dagger \rangle, \langle a_{-\mathbf{k}} a_{\mathbf{k}} \rangle, \langle a_{-\mathbf{k}} a_{-\mathbf{k}}^\dagger \rangle ]^T$ . As previously analyzed,  $\vec{G}_{\mathbf{k}} = \vec{G}_{\mathbf{k}}^a + \vec{G}_{\mathbf{k}}^b$  where  $\vec{G}_{\mathbf{k}}^{a(b)}$  is the correlation function corresponding to the marginal density matrix  $\rho_{a(b)}$  with the EOM

$$\frac{d}{dt} \begin{bmatrix} \vec{G}_{\mathbf{k}}^a \\ \vec{G}_{\mathbf{k}}^b \end{bmatrix} = \mathbb{L}_{\mathbf{k}}[f(t)] \begin{bmatrix} \vec{G}_{\mathbf{k}}^a \\ \vec{G}_{\mathbf{k}}^b \end{bmatrix} = \begin{bmatrix} \hat{\Gamma}_{\mathbf{k}}^a - \kappa \hat{\mathbf{1}} & \kappa \hat{\mathbf{1}} \\ \kappa \hat{\mathbf{1}} & \hat{\Gamma}_{\mathbf{k}}^b - \kappa \hat{\mathbf{1}} \end{bmatrix} \begin{bmatrix} \vec{G}_{\mathbf{k}}^a \\ \vec{G}_{\mathbf{k}}^b \end{bmatrix}, \quad (11)$$

where  $\hat{\mathbf{1}}$  is the unit matrix with dimension 4 and

$$\hat{\Gamma}_{\mathbf{k}}^{a(b)} = \begin{bmatrix} 0 & -\frac{i}{2} \delta_{\mathbf{k}}^{a(b)} & \frac{i}{2} \delta_{\mathbf{k}}^{a(b)} & 0 \\ \frac{i}{2} \delta_{\mathbf{k}}^{a(b)} & i(2 + \delta_{\mathbf{k}}^{a(b)}) & 0 & \frac{i}{2} \delta_{\mathbf{k}}^{a(b)} \\ -\frac{i}{2} \delta_{\mathbf{k}}^{a(b)} & 0 & -i(2 + \delta_{\mathbf{k}}^{a(b)}) & -\frac{i}{2} \delta_{\mathbf{k}}^{a(b)} \\ 0 & -\frac{i}{2} \delta_{\mathbf{k}}^{a(b)} & \frac{i}{2} \delta_{\mathbf{k}}^{a(b)} & 0 \end{bmatrix}, \quad (12)$$

in which  $\delta_{\mathbf{k}}^{a(b)} = r_{a(b)} + k^2 + Uf(t) - 1$  can be determined self-consistently during the time evolution.

*Ferromagnetic case.* If we start from the ground state in the ferromagnetic region, the  $O(N)$  symmetry has already spontaneously been broken from the beginning. Without loss of generality, we assume that symmetry is broken along the 1-direction in order parameter space, thus  $\phi_1(\mathbf{x})$  contains a

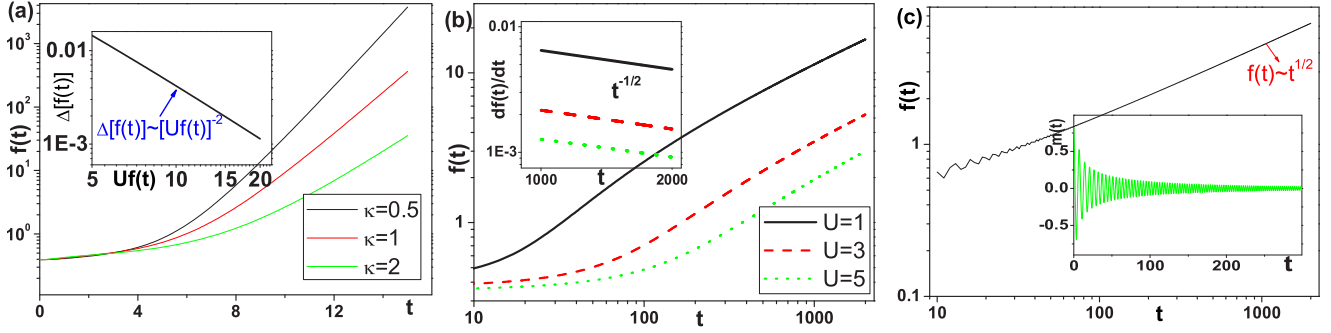


FIG. 4. (a) Time evolution of  $f(t)$  for the noninteracting case with parameters  $r_a = -r_b = 0.5$  (the inset is the gap of the instantaneous Liouville superoperator  $\mathbb{L}_k[f(t)]$  as a function of  $Uf(t)$  in the limit  $Uf(t) \gg r_{a(b)}$ ). (b) The dynamics of  $f(t)$  starting from the paramagnetic initial state with different  $U$  and  $r_a = -r_b = 0.5$ ,  $\kappa = 1$  [the inset is the long-time dynamics of  $\dot{f}(t)$ ]. (c) The dynamics of  $f(t)$  starting from the ferromagnetic initial state with  $U = 3$ ,  $r_a = -1.5$ ,  $r_b = -0.5$ , and  $\kappa = 1$  [the inset is the dynamics of the magnetization  $m(t)$ ], for (a)–(c)  $\Lambda = 5$ .

finite uniform magnetization  $m(t) = \langle \phi_1(\mathbf{x}) \rangle / \sqrt{N}$ , and the field  $\phi(\mathbf{k})$  can be expressed in terms of ladder operators as  $\phi_i(\mathbf{k}) = \frac{1}{\sqrt{2}}(a_{\mathbf{k}} + a_{-\mathbf{k}}^\dagger) + \delta_{i1}\phi_0(t)$  with  $\phi_0(t) = \sqrt{N}m(t)$  [70]. The corresponding self-consistent Hamiltonian takes the same form as that of the paramagnetic case Eq. (10), with the only difference that the  $\delta(t)$  in Eq. (10) is replaced by  $\tilde{\delta}(t) = r(t) + k^2 + U[\tilde{f}(t) + m^2(t)] - 1$ , where  $\tilde{f}(t) = \int d^d \mathbf{x} \sum_{i=2}^N \frac{1}{N} \langle \phi_i^2(\mathbf{x}) \rangle$ . The EOM of the correlation functions are similar to the paramagnetic case Eq. (11), with  $\delta_{\mathbf{k}}^{a(b)}$  replaced by  $\tilde{\delta}_{\mathbf{k}}^{a(b)} = r_{a(b)} + k^2 + U[\tilde{f}(t) + m^2(t)] - 1$ , and the EOM for the magnetization  $m(t)$  can be obtained from that for  $\phi_0^{a(b)}$ :

$$\frac{d}{dt} \begin{bmatrix} \langle \phi_0^a \rangle \\ \langle \pi_0^a \rangle \\ \langle \phi_0^b \rangle \\ \langle \pi_0^b \rangle \end{bmatrix} = \begin{bmatrix} -\kappa & 1 & \kappa & 0 \\ -\tilde{\delta}_0^a & -\kappa & 0 & \kappa \\ \kappa & 0 & -\kappa & 1 \\ 0 & \kappa & -\tilde{\delta}_0^b & -\kappa \end{bmatrix} \begin{bmatrix} \langle \phi_0^a \rangle \\ \langle \pi_0^a \rangle \\ \langle \phi_0^b \rangle \\ \langle \pi_0^b \rangle \end{bmatrix}, \quad (13)$$

where  $\sqrt{N}m(t) = \langle \phi_0 \rangle = \langle \phi_0^a \rangle + \langle \phi_0^b \rangle$ .

**Results.** We first focus on the noninteracting case ( $U = 0$ ), as shown in Fig. 4(a). This bosonic system with a locally unbounded Hilbert space will absorb energy indefinitely, which leads to exponentially divergent dynamics due to the parametric resonance between the external driving and the selected momentum modes of the Hamiltonian. Mathematically, the exponential divergence indicates a positive branch in the spectrum of the Liouville superoperator  $\mathbb{L}_k$  defined in Eq. (11), as shown in the inset of Fig. 4(a). In the presence of interaction ( $U > 0$ ), we find that even though the dynamics are still divergent with time, the interaction will fundamentally change the divergence from an exponential to an algebraic one in the long-time dynamics:  $f(t) \sim t^\eta$ , where again the exponent  $\eta = 0.5$  is universal and independent of the details of the systems, e.g., the parameters in the Hamiltonian and external driving, the strength of the interaction, as well as the choices of the initial state, as shown in Figs. 4(b) and 4(c). Physically, this means that in the quantum  $O(N)$  model in the large- $N$  limit, the (repulsive) interaction will significantly suppress the driving-induced heating dynamics through a nonlinear effect: the divergence of  $f(t)$  will increase the effective mass of the system which makes the system less and less sensitive to the

external driving. Mathematically, the EOM of each  $k$  mode is determined by  $\Delta_k$ :

$$df_{\mathbf{k}}(t)/dt = \Delta_{\mathbf{k}}[f(t)]f_{\mathbf{k}}(t), \quad (14)$$

where the gap  $\Delta_{\mathbf{k}}$  is the real part of the positive eigenvalue of the instantaneous Liouville superoperator  $\mathbb{L}_k[f(t)]$  defined in Eq. (11). Different modes are coupled through the relation  $f(t) = \int_{\mathbf{k}} f_{\mathbf{k}}(t)$ . Since  $f(t)$  diverges with time, in the long-time limit we have  $Uf(t) \gg r_{a(b)} + \Lambda^2$  and  $\delta_{\mathbf{k}}^{a(b)} \approx Uf(t) \pm \delta r$ , where  $\delta r = (r_a - r_b)/2 \ll Uf(t)$ . In this limit, we numerically calculate the gap of the instantaneous Liouville superoperator [see the inset of Fig. 4(a)], and find the asymptotic relation between the gap and  $f(t)$ :  $\Delta_{\mathbf{k}}[f(t)] \propto 1/[Uf(t)]^2$ . Hence, we can obtain the EOM of  $f(t)$  in the long-time limit as

$$df(t)/dt \propto 1/[U^2 f(t)] \quad (15)$$

with the asymptotic solution  $f(t) \sim t^{1/2}$  for  $t \rightarrow \infty$ . For the ferromagnetic case, we can find that in the long-time limit, the spontaneous magnetization is destroyed by external stochastic driving;  $m(t) \rightarrow 0$  as shown in the inset of Fig. 4(c). Therefore, the long-time behavior if we start from a ferromagnetic initial state is qualitatively the same as if starting from the paramagnetic case.

## V. EXPERIMENTAL REALIZATION

In this section, we will briefly discuss the possible experimental realization of the above two models as well as the consequence of the imperfection in the realistic experimental systems. The 1D spinless fermionic model with a stochastically fluctuating staggered potential can be realized by loading ultracold fermions (or hard-core bosons) into a quasi-1D optical superlattice potential, which can be implemented by overlaying two commensurate lattices generated by lasers at the wavelengths of  $\lambda$  and  $2\lambda$ . The telegraph-like stochastic driving can be artificially introduced in a controlled way by programmable tuning of the relative strength of the two laser beams during the time evolution. In Sec. III, we focus on the population imbalance between the two sublattices, which can be measured directly by employing a band-mapping and imaging technique [5,71]. In the optical lattice, the Kitaev

chain discussed in Sec. III can be implemented by employing a Raman-induced dissociation technique and immersing the system into an atomic BCS reservoir formed by Feshbach molecules [72–74]. The static disorder has been created optically by using speckle patterns [75], and the NN interactions naturally exist in magnetic dipolar atomic systems in optical lattices. In recent experiments with erbium atoms [76], it was measured that the strength of the NN interaction ( $V/\hbar \simeq 30$  Hz for a lattice constant  $a_0 = 266$  nm) is of the same order of magnitude as that of the single-particle hopping amplitude ( $J/\hbar \simeq 30 \sim 100$  Hz depending on the lattice depths). The parameters encountered in the experiment typically meet the parameter regime studied previously.

In realistic systems, the experimental imperfection will make the system deviate from the ideal case we studied above and now we discuss their effect on the long-time behavior. One of the most important imperfection in optical lattice system is the nonhomogeneous external potential due to the external trap, which breaks the translational symmetry and couples different  $k$  modes via a single-particle scattering process similar with the disorder case; thus it may have important consequence for the long-time dynamics. In Appendix D, we numerically analyze this problem and find that the harmonic trap will induce a faster power-law decay  $t^{-\eta}$ , where the exponent  $\eta = 2$  independently of the strength of the harmonic trap. Even though the harmonic trap qualitatively changes the long-time dynamics, as we show in Appendix D, the diffusive long-time behavior  $t^{-0.5}$  in the ideal case can still be observed in a potential of an optical box trap [77].

The second imperfection we discuss here is the interband coupling: in the realistic systems the stochastic driving will continuously heat the system and pump the particle to the higher orbital bands after sufficiently long time, which makes the single-band approximation invalid. However, as long as the band gap  $\Delta$  is large enough, the effective interband coupling is suppressed by the band gap via a second-order perturbation process ( $J_{\text{eff}} \sim J'^2/\Delta$  with  $J'$  the interband coupling), and its effect can be observed on a long time scale  $t > 1/J_{\text{eff}}$ . Therefore, the “long-time” behavior defined in the ideal case can be considered as an intermediate time region  $1/J \ll t \ll 1/J_{\text{eff}}$  in a realistic experimental system with large band gap. Another common perturbation in the optical lattice setup is the noise, which is inevitable due to the impurity of the laser beams. In the Appendix D, we show that the white noise will not qualitatively change the long-time behavior of the stochastically driven model. Finally we discuss the finite-temperature effect. Even though temperature is not well defined during the nonequilibrium dynamics, it can indeed affect the preparation of the initial state. However, throughout this paper, we focus on the long-time behavior of the system, where the initial state information has been washed out by the external driving; thus finite-temperature effects are irrelevant for our results.

The connection between the discussion in Sec. IV and realistic experimental systems is subtle, since any realistic system has an upper bound of the locally Hilbert space. However, for those systems with a sufficient large local Hilbert space, e.g., the multicomponent Bose-Hubbard model with a large component number and high filling factors, we conjecture that the long-time behavior discussed in Sec. IV can

capture the correct intermediate-time dynamics during which the information of the initial state has been lost but the energy of the system is still far from its upper bound, because during this time period the system can absorb energy “infinitely” without feeling the restriction imposed by the upper bound of the local Hilbert space.

## VI. CONCLUSION AND OUTLOOK

In this paper, we study the long-time behavior of stochastically driven quantum many-body systems based on two representative examples, and special attention is devoted to the effect of the mode-coupling terms, especially the interactions. As a conclusion of this paper, we wish to emphasize some connections and differences of our results with other relevant ones and provide an outlook. First, even though many of the phenomena we observed above have analogs in classic physics (e.g., the power-law behavior  $t^{-1/2}$  corresponds to the classic diffusive dynamics), we should emphasize that our system is essentially quantum instead of classic even near the infinite-temperature state. However, this fact does not preclude the possibility of a more universal physical origin behind these phenomena, independently of the quantum or classic features of the systems, and is worthy of investigation in the future. Moreover, the stochastically driven systems studied above differ from another well-studied problem, quantum many-body systems subject to white noise, in two aspects: the external driving is spatially homogeneous instead of site-dependent, and the correlation time of the stochastic force is finite ( $1/\kappa$ ) rather than zero. These differences give rise to significant consequences; e.g., it is known that for a 1D XXZ model subject to white noise, the  $U(1)$  symmetry-breaking term is a relevant perturbation for the long-time behavior while the NN interaction is not [26], which is exactly the opposite of our observation in the stochastic driving cases.

By considering specific examples, we have taken the first step towards characterizing the long-time dynamics of stochastically driven interacting quantum systems, but a comprehensive understanding of this problem is far from achieved. Some avenues for further work immediately suggest themselves. The first and most important question is the generality of the above results. Even though we have tried to generalize our results as much as we could by choosing various representative system Hamiltonians, driving protocols, and mode-coupling mechanisms, there is no guarantee that the above results can hold for any stochastically driven quantum many-body systems. A systematic answer to this question requires us to treat the infinite-temperature state as a fixed point and develop an effective nonequilibrium field theory to characterize the dynamics towards the fixed point, and determine the relevancy of various perturbations through a controllable renormalization group analysis, which is beyond the scope of this work and will be left for the future. From the numerical point of view, to approach the long-time behavior for a large system, it would be important to develop efficient numerical methods based, e.g., on the density matrix renormalization group (DMRG) technique [78,79] to directly solve the master equation (2) instead of doing the ensemble average over all the stochastic trajectories. Another



important factor we have not considered in this paper is the dissipation, which is inevitable for almost all the quantum systems. The dissipation will balance the energy intake from the stochastic driving, and thus can lead to a nontrivial steady state other than the infinite-temperature state we studied above. However, for a system with sufficiently weak dissipation (e.g., a well-isolated optical lattice system), we may expect that the “long-time” behavior we studied in the dissipationless case actually corresponds to an intermediate-time region ( $1/J \ll t \ll 1/\gamma$  with  $\gamma$  the dissipation strength) which is long enough for the stochastic driving to wash out the initial state information, but sufficiently short compared to the time scale after which the dissipation will take over the evolutions. However, for a system whose dissipation is compatible with the energy scale in the system Hamiltonian [ $\gamma \sim O(J)$ ], both the steady state and the long-time dynamics may be much more complex and such a driven-dissipative system (e.g., Ref. [80]), even though beyond the scope of this work, is one of the most important avenues for further studies.

#### ACKNOWLEDGMENTS

Z.C. wishes to thank P. Zoller for raising our interest in the problem of stochastically driven quantum many-body systems and for many stimulating discussions and valuable suggestions during the work. We wish to thank M. A. Baranov and Ying Hu for fruitful discussions. Z.C. acknowledges support from the National Key Research and Development Program of China (Grant No. 2016YFA0302001) the NSF of China under Grant No. 11674221 and the Shanghai Rising-Star Program. C.H. acknowledges support from the Nanosystems Initiative Munich (NIM) and the ExQM graduate school of the Elitenetzwerk Bayern. This work is supported by the Austrian Science Fund through SFB FOQUS (FWF Project No. F4006-N16) and the ERC Synergy Grant UQUAM.

#### APPENDIX A: DERIVATION OF THE EOM OF THE MARGINAL DENSITY MATRIX

In this Appendix we will derive the EOM of the marginal density matrix [Eq. (1) in the paper]. To do that, we first discretize the time axis (from  $t_0$  to  $t_n$ ) into small slices of size  $dt = (t_n - t_0)/n$ , and we denote  $t_k = t_0 + kdt$  with  $k$  an integer from 0 to  $n$ . For  $n \rightarrow \infty$ , we can assume that the jump of the parameter  $\lambda$  can only take place at the discrete time  $t_k$ . We further denote  $\{\lambda_n\} = \{\lambda_1 \cdots \lambda_{n-1}\}$  as a trajectory of the fluctuating parameter  $\lambda(t)$ , which satisfies  $\lambda(t_k) = \lambda_k$  for  $k = 0, \dots, n-1$  and  $\lambda_k = \lambda_a$  or  $\lambda_b$ . For a given trajectory  $\{\lambda_n\}$ , we can define its probability  $P_{\{\lambda_n\}} = P(\lambda(t_{n-1}) = \lambda_{n-1}, t_{n-1}; \dots; \lambda(t_0) = \lambda_0, t_0)$ , and the density matrix at  $t_n$  following this trajectory as  $\rho_{\{\lambda_n\}}(t_n) = \mathcal{U}_{\{\lambda_n\}} \rho(t_0) \mathcal{U}_{\{\lambda_n\}}^{-1}$ , with the corresponding unitary evolution operators:  $\mathcal{U}_{\{\lambda_n\}} = e^{idt H_{\lambda_{n-1}}} \cdots e^{idt H_{\lambda_0}}$ . With these definitions, we obtain the density matrix after the ensemble average of all the trajectories:

$$\rho_s(t_n) = \sum_{\{\lambda_n\}} P_{\{\lambda_n\}} \rho_{\{\lambda_n\}}(t_n). \quad (\text{A1})$$

The corresponding marginal density matrix  $\rho_{a(b)}(t_n) = \langle \rho(t_n) \delta(\lambda(t_{n-1}) = \lambda_{a(b)}) \rangle$  can be expressed as

$$\rho_a(t_n) = \sum_{\{\lambda_{n-1}\}} P(\lambda_a, t_{n-1} | \lambda_{n-2}, t_{n-2}) P_{\{\lambda_{n-1}\}} \times e^{idt H_a} \rho_{\{\lambda_{n-1}\}}(t_{n-1}) e^{-idt H_a}, \quad (\text{A2})$$

where  $P(\lambda_a, t_{n-1} | \lambda_{n-2}, t_{n-2})$  denotes the conditional probability of the case that  $\lambda(t_{n-1})$  takes the value of  $\lambda_a$  if  $\lambda(t_{n-2}) = \lambda_{n-2}$ . To express  $\rho_a(t_n)$  in terms of  $\rho_a(t_{n-1})$  and  $\rho_b(t_{n-1})$ , we further expand the summation over  $\lambda_{n-2}$  in Eq. (A2) and obtain

$$\rho_a(t_n) = P(\lambda_a, t_{n-1} | \lambda_a, t_{n-2}) e^{idt H_a} \rho_a(t_{n-1}) e^{-idt H_a} + P(\lambda_a, t_{n-1} | \lambda_b, t_{n-2}) e^{idt H_a} \rho_b(t_{n-1}) e^{-idt H_a}. \quad (\text{A3})$$

We use that in the time interval  $[t_n, t_{n-1}]$  the transition probability for the parameter  $\lambda(t)$  is  $\kappa dt$ , which indicates that  $P(\lambda_a, t_{n-1} | \lambda_a, t_{n-2}) = 1 - \kappa dt$  and  $P(\lambda_a, t_{n-1} | \lambda_b, t_{n-2}) = \kappa dt$ . In the limit of  $dt \rightarrow 0$ , we can expand the right-hand side of Eq. (A3) to the first order in  $dt$  and obtain

$$\frac{\rho_a(t_n) - \rho_a(t_{n-1})}{dt} = i[\rho_a(t_{n-1}), H_a] - \kappa \rho_a(t_{n-1}) + \kappa \rho_b(t_{n-1}),$$

which reduces to the EOM of the marginal density matrix  $\rho_a(t)$ , Eq. (1) in the paper, in the limit  $dt \rightarrow 0$  [the EOM of  $\rho_b(t)$  can be obtained similarly].

#### APPENDIX B: DETAILS OF NUMERICAL METHODS

In Sec. III, to study the time evolution of the system, we used two methods: the marginal density matrix method (MDMM) for small system sizes ( $L \leq 12$ ) and the unitary evolution method (UEM) for larger ones ( $L = 16$ ). In this appendix, we provide some details about these two methods, and check the numerical convergence of the results. We also numerically verify that the MDMM is equivalent to UEM for a sufficiently large number of sampled trajectories.

*Unitary evolution method.* For a given trajectory, the time evolution is unitary under a time-dependent Hamiltonian  $H(\{\lambda(t)\})$ ; thus at time  $t$  the wave function can be expressed as

$$|\Psi(t)\rangle = \mathcal{T} e^{-i \int_0^t H(\lambda(t')) dt'} |\Psi(0)\rangle = \prod_n e^{-i H_n \delta t} |\Psi(0)\rangle, \quad (\text{B1})$$

where  $\mathcal{T}$  is the time ordering operator,  $\delta t = t/N$  is the time interval, and  $H_n = H(\lambda(t_n))$  is the Hamiltonian at  $t_n$ . To calculate the time evolution, it is more convenient to decompose the total Hamiltonian into pieces that act only on odd bonds and even bonds,

$$H_n = H_{\text{even}}^n + H_{\text{odd}}^n, \quad (\text{B2})$$

where  $H_{\text{odd}}^n = \sum_i H_{2i-1, 2i}^n$  and  $H_{\text{even}}^n = \sum_i H_{2i, 2i+1}^n$ . All the terms within the summation of  $H_{\text{odd}}$  or  $H_{\text{even}}$  commute with each other. For each time step, the evolution operator can be expanded in a second-order Suzuki-Trotter expansion:

$$e^{-i H_n \delta t} = e^{-i H_{\text{even}}^n \delta t / 2} e^{-i H_{\text{odd}}^n \delta t} e^{-i H_{\text{even}}^n \delta t / 2} + O(\delta t^3).$$

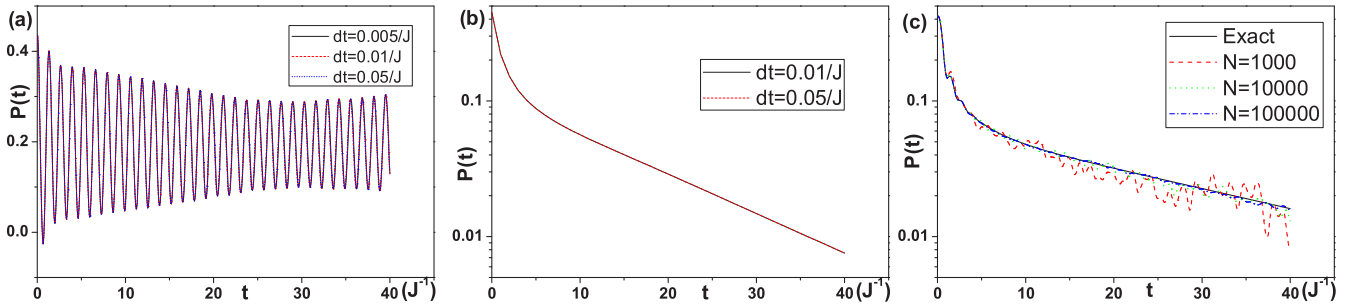


FIG. 5. Convergence check of the dependence of results on (a) the time step  $\delta t$  in UEM with  $V = J, L = 16$ ; (b)  $\delta t$  in the MDMM with  $V = 0.2J, L = 12$ ; and (c) the number of the sampled trajectories  $N$  in UEM with  $V = 0, L = 16$ . In (a)–(c) we choose  $\delta = 2J, \kappa = 2J$ .

For each bond, we can decompose the Hamiltonian into the diagonal and off-diagonal parts:

$$H_{i,i+1}^n = H_{i,i+1}^d + H_{i,i+1}^o, \quad (\text{B3})$$

where in our case  $H_{i,i+1}^o = -J(c_i^\dagger c_{i+1} + \text{H.c.})$  and  $H_{i,i+1}^d = V n_i n_{i+1} + \frac{\lambda(t)}{2} (-1)^i (n_i - n_{i+1})$ . Thus for each bond the evolution operator can be further decomposed as

$$e^{-iH_{i,i+1}^n \delta t} = e^{-iH_{i,i+1}^d \delta t/2} e^{-iH_{i,i+1}^o \delta t} e^{-iH_{i,i+1}^d \delta t/2} + O(\delta t^3),$$

where  $e^{-iH_{i,i+1}^d \delta t/2}$  is a diagonal matrix, and  $e^{-iH_{i,i+1}^o}$  only operates on two adjacent sites  $i$  and  $i + 1$ . Hence, its operation on the wave function can be easily performed without explicitly calculating the matrix  $e^{-iH_{i,i+1}^o}$ .

In our simulation of the  $L = 16$  system using UEM, we choose the time interval  $\delta t = 0.005J^{-1}$ . Since the second Trotter decomposition we used gives the errors of third order of the time step  $\delta t$ , it is necessary to check the numerical convergence of our results in the  $\delta t$  we used. To do this, we choose the unitary evolution under one of the simplest trajectories with only one flipping of the parameters at  $t = 0$  (quantum quench problem). The convergence analysis is shown in Fig. 5(a).

*Marginal density matrix method.* For small systems, we can directly solve the EOM of the marginal density matrix Eq. (3), which is a linear differential equation, using a fourth-order Runge-Kutta method, whose accuracy also depends on the time interval  $\delta t$ . In our simulation using MDMM, we choose  $\delta t = 0.05J^{-1}$ , and the convergence analysis is shown in Fig. 5(b). Notice that the  $\delta t$  we choose in UEM is much smaller than that in the MDMM. The reason is that in the unitary evolution the error introduced by the finite  $\delta t$  in the Trotter decomposition will accumulate during the time evolution, and will eventually make the simulation inaccurate, while in MDMM, the evolution is not unitary and it will converge to a steady state. This convergence provides a self-correction mechanism for the accumulated error in the long-time evolution, thus allowing us to use larger  $\delta t$ .

*Equivalence of the two methods.* In the last section, we provide an analytic proof of the equivalence between the above two methods. Here, we will numerically verify that the MDMM is equivalent to UEM for a sufficiently large number of sampled trajectories (in our simulation of  $L = 16$  using UEM, we choose  $\mathcal{N} = 10^5$ ). As shown in Fig. 5(c), the results of UEM will converge to that of MDMM with increasing

number of sampled trajectories ( $\mathcal{N}$ ), and for  $\mathcal{N} \sim 10^5$ , the results of the two methods almost coincide.

### APPENDIX C: SIGNIFICANT OTHERS

In this Appendix, we consider another stochastically driven fermionic model, which exhibits a dynamical phase transition between phases with algebraic and exponential relaxation behavior absent in the one previously studied in Sec. III. Also we propose a sufficient condition for the existence of the algebraic relaxation behavior in general quadratic fermionic systems with stochastic driving.

*Dynamical phase transition.* The model we consider is a 1D spin-1/2 fermionic model with a spin-flip term in a Zeeman field with the Hamiltonian

$$H = \sum_i \left[ \sum_\sigma (-J_\sigma c_{i\sigma}^\dagger c_{i+1\sigma} + \text{H.c.}) - h_z (n_{i\uparrow} - n_{i\downarrow}) + \lambda(t) (c_{i\uparrow}^\dagger c_{i\downarrow} + \text{H.c.}) \right], \quad (\text{C1})$$

where  $\sigma = \uparrow, \downarrow$  denotes the spin index,  $J_\sigma$  is the spin-dependent hopping amplitude,  $h_z$  is the Zeeman field, and  $\lambda(t)$  is the stochastic driving parameter with transition between two values  $\lambda_a$  and  $\lambda_b$  during the time evolution. Assuming  $J_\uparrow = -J_\downarrow = J$  in the following, we focus on dynamics of the quantity  $\Delta E(t) = E(t) - E_0$  to monitor the long-time behavior, where  $E(t) = \text{Tr} \rho_s(t) \bar{H}$  with  $\bar{H} = (H_a + H_b)/2$  is the time-independent Hamiltonian and  $E_0 = E(t \rightarrow \infty)$  is the energy at the infinite-temperature state (steady state). The long-time behavior of  $\Delta E(t)$  characterizes how the system approaches the steady state.

The dynamics of  $\Delta E(t)$  is plotted in Fig. 6(a), where we find that for  $h_z < 2J$ , the long-time behavior is similar to that given before,  $\Delta E(t) \sim t^{-\frac{1}{2}}$ , while at the point  $h_z = 2J$ , it suddenly turns to  $\Delta E(t) \sim t^{-\frac{1}{4}}$ . Beyond this point  $h_z > 2J$ , an exponential decay takes place:  $\Delta E(t) \sim e^{-\gamma(h_z)t}$ . As previously pointed out, in the absence of interactions, the long-time behavior is determined by the Liouville spectrum  $\mathbb{L}_k$ . In Fig. 6(b), we plot the Liouville gap  $\Delta_k$ , which shows that in the region  $0 < h_z < 2J$ , the gapless point is shifted from  $k_c = \pi/2$  to  $\pi$ , while around the gapless point,  $\Delta_k$  can always be expanded as  $\Delta_k = \alpha \delta k^2 + O(\delta k^4)$  with  $\delta k = k - k_c$ , which is responsible for the algebraic behavior  $\Delta E(t) \sim t^{-\frac{1}{2}}$ . At the critical point ( $h_z = 2J$ ), the coefficient

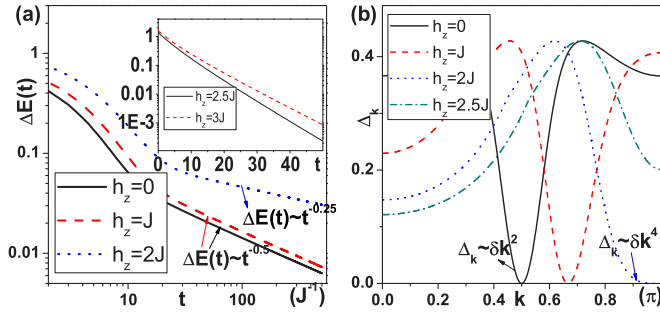


FIG. 6. (a) Dynamics of the stochastically driven spin-1/2 fermionic model [Eq. (C1)] in algebraic and exponential (the inset) regions. (b) The Liouville gap  $\Delta_k$  for different  $h_z$ . We choose  $\lambda_1 = 0$ ,  $\lambda_2 = J$ , and  $\kappa = 2J$ .

before the quadratic term vanishes ( $\alpha = 0$ ) and the quartic term dominates ( $\Delta_k = \eta\delta k^4$ ). By performing a similar integral to that in Eq. (5), we can obtain  $\Delta E(t) \sim t^{-1/4}$ . For  $h_z > 2J$ , a gap is opened indicating an exponential decay. In summary, we propose a stochastically driven model exhibiting a dynamical phase transition, which is supplementary to various long-time behaviors in the case previously studied in Sec. III. Since the steady states are the same for both phases, this phase transition can only be characterized by the dynamical instead of static properties, e.g., the relaxation time, as well as the singularity of the Liouville gap at the transition point. Notice that the dynamical phase transition we proposed here has a subtle difference from its conventional definition in which the singularity occurs during the time evolution [81–83].

This dynamic phase transition can be understood by the sufficient condition for the existence of the algebraic relaxation we proposed in Sec. III. For  $h_z < 2J$ , we can always find a  $k_c = \cos^{-1} \frac{h_z}{2J}$  where  $\hat{H}_1(k_c) = 0$  thus commutes with  $\hat{H}_2(k_c)$ , while for  $h_z > 2J$ ,  $[H_1(k), H_2(k)] \neq 0$  for all  $k$ , thus opening a finite Liouville gap which leads to an exponential decay.

#### APPENDIX D: EFFECT OF THE EXPERIMENTAL IMPERFECTIONS

In this Appendix, we analyze the effect of the experimental imperfections on the long-time dynamics of the stochastically

driven spinless fermion model in the optical lattice system. We first examine the effect of the external potential. We choose two common potentials in ultracold atomic experiments: the harmonic trap and box trap. The Hamiltonian of the system reads

$$H = H_0 + \sum_i V_i n_i, \quad (\text{D1})$$

where  $H_0$  is the same as Eq. (4),  $V_i = \frac{1}{2}\omega^2(i - L/2)^2$  corresponds to the harmonic trap, while for the box trap we choose  $V_i = V_0$  for  $|i| \leq L_0$  and  $V_i = 0$  for  $|i| > L_0$ . As shown in Fig. 7, in the presence of the harmonic trap, the scattering between the particle and the external potential will induce a faster power-law decay  $t^{-\eta}$ , where the exponent  $\eta = 2$  independently of the strength of the harmonic trap, while for the box trap, the scattering only occurs at two points  $i = \pm L_0$ , and thus does not qualitatively change the long-time behavior  $t^{-1/2}$  we found in the ideal case.

Now we analyze the effect of the white noise, which provides another stochastic process independent of the driving force. The Hamiltonian of the white noise can be written as  $H' = \sum_i \xi_i(t) n_i$ , where  $\xi_i(t)$  represents the site-dependent random field satisfying  $\langle \xi_i(t) \xi_j(t') \rangle = \sqrt{\gamma} \delta_{ij} \delta(t - t')$ . In spite of the stochastic properties, the white noise differs from the previously studied stochastic driving in two aspects: it is site-dependent and with zero correlation length. The ensemble average over the external white noise can be performed following the standard procedure [19], and the EOM of the marginal density matrix reads

$$\begin{aligned} \frac{d\rho_a(t)}{dt} &= i[\rho_a, \hat{H}_a] + \hat{\mathcal{D}}\rho_a - \kappa\rho_a + \kappa\rho_b, \\ \frac{d\rho_b(t)}{dt} &= i[\rho_b, \hat{H}_b] + \hat{\mathcal{D}}\rho_b + \kappa\rho_a - \kappa\rho_b, \end{aligned} \quad (\text{D2})$$

where  $\hat{\mathcal{D}}\rho = \sum_i \gamma [n_i \rho n_i - \frac{1}{2}(n_i^2 \rho + \rho n_i^2)]$  represents the effect of the white noise. Since it is still a translationally invariant and noninteracting system, the dynamics of  $P(t)$  can be easily solved based on Eq. (D2). As shown in Fig. 7(b), we can find that even though the external white noise makes the system decay faster since it facilitates the heating, the long-time behavior is still qualitatively the same as that in the noise-free

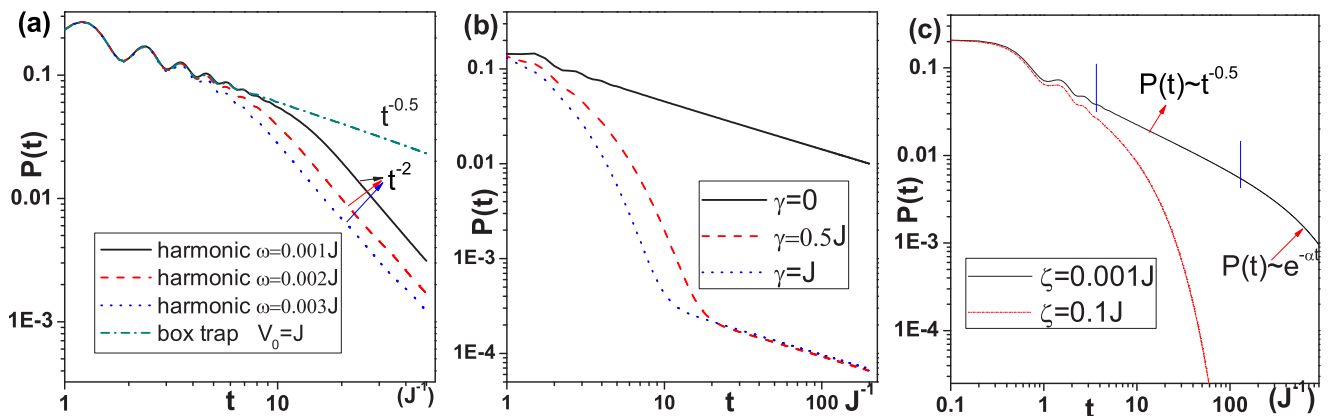


FIG. 7. Dynamics of the stochastically driven spinless fermionic model in the presence of (a) external trap, (b) white noise, and (c) dissipation with parameters  $\lambda_1 = 0$ ,  $\lambda_2 = J$ , and  $\kappa = 2J$ . In (a) we choose  $L = 120$  and  $L_0 = L/4$  for the box trap.

case  $P(t) \sim t^{-0.5}$ . This indicates that the white noise is an irrelevant perturbation for the long-time behavior.

Finally, we discuss the effect of dissipation, which is inevitable in almost all the experimental setups. We consider one of the most common dissipation mechanisms in ultracold atomic experiments: the single-particle loss that a particle in the optical lattice can escape from the system into the environment. We further assume that the environment satisfies the Born-Markovian approximation; thus the EOM of the marginal density matrix is similar to Eq. (D2), but the dissipative operator is replaced by  $\hat{D}'\rho = \zeta \sum_i [c_i \rho c_i^\dagger - \frac{1}{2}(c_i^\dagger c_i \rho +$

$\rho c_i^\dagger c_i)]$  with  $\zeta$  the strength of the dissipation. In this case, the EOM of the stochastically driven dissipative fermionic model can still be solved exactly. The time evolution of  $P(t)$  is shown in Fig. 7(c), from which we can find that for weak dissipation  $\zeta \ll J$ , the universal algebraic decay  $P(t) \sim t^{-0.5}$  occurs in the intermediate time regime  $1/J \ll t \ll 1/\zeta$ , while the dissipation dominates after sufficiently long time  $t \gg 1/\zeta$  and gives rise to an exponential decay, which agrees with our analysis in the main text. When the dissipation strength is compatible with the energy scale in the system, such an intermediate regime vanishes.

- 
- [1] J. Eisert, M. Friesdorf, and C. Gogolin, Quantum many-body systems out of equilibrium, *Nat. Phys.* **11**, 124 (2015).
- [2] M. Rigol, V. Dunjko, and M. Olshanii, Thermalization and its mechanism for generic isolated quantum systems, *Nature (London)* **452**, 854 (2008).
- [3] A. Polkovnikov, K. Sengupta, A. Silva, and M. Vengalattore, Colloquium: Nonequilibrium dynamics of closed interacting quantum systems, *Rev. Mod. Phys.* **83**, 863 (2011).
- [4] M. Gring, M. Kuhnert, T. Langen, T. Kitagawa, B. Rauer, M. Schreitl, I. Mazets, D. A. Smith, E. Demler, and J. Schmiedmayer, Relaxation and prethermalization in an isolated quantum system, *Science* **337**, 1318 (2012).
- [5] S. Trotzky, Y.-A. Chen, A. Flesch, I. P. McCulloch, U. Schollwöck, J. Eisert, and I. Bloch, Probing the relaxation towards equilibrium in an isolated strongly correlated one-dimensional Bose gas, *Nat. Phys.* **8**, 325 (2012).
- [6] L. D'Alessio, Y. Kafri, A. Polkovnikov, and M. Rigol, From quantum chaos and eigenstate thermalization to statistical mechanics and thermodynamics, *Adv. Phys.* **65**, 239 (2016).
- [7] S. Braun, M. Friesdorf, S. S. Hodgman, M. Schreiber, J. P. Ronzheimer, A. Riera, M. del Rey, I. Bloch, J. Eisert, and U. Schneider, Emergence of coherence and the dynamics of quantum phase transitions, *Proc. Natl. Acad. Sci. USA* **112**, 3641 (2015).
- [8] J. Struck, C. Ölschläger, R. Le Targat, P. Soltan-Panahi, A. Eckardt, M. Lewenstein, P. Windpassinger, and K. Sengstock, Quantum simulation of frustrated classical magnetism in triangular optical lattices, *Science* **333**, 996 (2011).
- [9] J. Struck, C. Ölschläger, M. Weinberg, P. Hauke, J. Simonet, A. Eckardt, M. Lewenstein, K. Sengstock, and P. Windpassinger, Tunable Gauge Potential for Neutral and Spinless Particles in Driven Optical Lattices, *Phys. Rev. Lett.* **108**, 225304 (2012).
- [10] G. Jotzu, M. Messer, R. Desbuquois, M. Lebrat, T. Uehlinger, D. Greif, and T. Esslinger, Experimental realization of the topological Haldane model with ultracold fermions, *Nature (London)* **515**, 237 (2014).
- [11] S. Diehl, A. Micheli, A. Kantian, B. Kraus, H. P. Büchler, and P. Zoller, Quantum states and phases in driven open quantum systems with cold atoms, *Nat. Phys.* **4**, 878 (2008).
- [12] M. M. Wolf, F. Verstraete, and J. I. Cirac, Quantum computation and quantum-state engineering driven by dissipation, *Nat. Phys.* **5**, 633 (2009).
- [13] A. J. Daley, J. M. Taylor, S. Diehl, M. Baranov, and P. Zoller, Atomic Three-Body Loss as a Dynamical Three-Body Interaction, *Phys. Rev. Lett.* **102**, 040402 (2009).
- [14] J. T. Barreiro, M. Müller, P. Schindler, D. Nigg, T. Monz, M. Chwalla, M. Hennrich, C. F. Roos, P. Zoller, and R. Blatt, An open-system quantum simulator with trapped ions, *Nature (London)* **470**, 486 (2011).
- [15] S. Diehl, E. Rico, M. A. Baranov, and P. Zoller, Topology by dissipation in atomic quantum wires, *Nat. Phys.* **7**, 971 (2011).
- [16] M. A. Cazalilla, F. Sols, and F. Guinea, Dissipation-Driven Quantum Phase Transitions in a Tomonaga-Luttinger Liquid Electrostatically Coupled to a Metallic Gate, *Phys. Rev. Lett.* **97**, 076401 (2006).
- [17] T. Prosen and I. Pižorn, Quantum Phase Transition in a Far-from-Equilibrium Steady State of an  $xy$  Spin Chain, *Phys. Rev. Lett.* **101**, 105701 (2008).
- [18] T. Prosen, Exact Nonequilibrium Steady State of a Strongly Driven Open  $xxz$  Chain, *Phys. Rev. Lett.* **107**, 137201 (2011).
- [19] B. Horstmann, J. I. Cirac, and G. Giedke, Noise-driven dynamics and phase transitions in fermionic systems, *Phys. Rev. A* **87**, 012108 (2013).
- [20] A. Rancon, C.-L. Hung, C. Chin, and K. Levin, Quench dynamics in Bose-Einstein condensates in the presence of a bath: Theory and experiment, *Phys. Rev. A* **88**, 031601(R) (2013).
- [21] Z. Cai, U. Schollwöck, and L. Pollet, Identifying a Bath-Induced Bose Liquid in Interacting Spin-Boson Models, *Phys. Rev. Lett.* **113**, 260403 (2014).
- [22] M. Žnidarič, Relaxation times of dissipative many-body quantum systems, *Phys. Rev. E* **92**, 042143 (2015).
- [23] E. G. Dalla Torre, E. Demler, T. Giamarchi, and E. Altman, Quantum critical states and phase transitions in the presence of non-equilibrium noise, *Nat. Phys.* **6**, 806 (2010).
- [24] J. Marino and A. Silva, Relaxation, prethermalization, and diffusion in a noisy quantum Ising chain, *Phys. Rev. B* **86**, 060408 (2012).
- [25] D. Poletti, J.-S. Bernier, A. Georges, and C. Kollath, Interaction-Induced Impeding of Decoherence and Anomalous Diffusion, *Phys. Rev. Lett.* **109**, 045302 (2012).
- [26] Z. Cai and T. Barthel, Algebraic Versus Exponential Decoherence in Dissipative Many-Particle Systems, *Phys. Rev. Lett.* **111**, 150403 (2013).
- [27] L. M. Sieberer, S. D. Huber, E. Altman, and S. Diehl, Dynamical Critical Phenomena in Driven-Dissipative Systems, *Phys. Rev. Lett.* **110**, 195301 (2013).
- [28] M. Buchhold and S. Diehl, Nonequilibrium universality in the heating dynamics of interacting Luttinger liquids, *Phys. Rev. A* **92**, 013603 (2015).

- [29] J. Marino and S. Diehl, Driven Markovian Quantum Criticality, *Phys. Rev. Lett.* **116**, 070407 (2016).
- [30] J. Marino and S. Diehl, Quantum dynamical field theory for nonequilibrium phase transitions in driven open systems, *Phys. Rev. B* **94**, 085150 (2016).
- [31] T. Kitagawa, E. Berg, M. Rudner, and E. Demler, Topological characterization of periodically driven quantum systems, *Phys. Rev. B* **82**, 235114 (2010).
- [32] N. H. Lindner, G. Refael, and V. Galitski, Floquet topological insulator in semiconductor quantum wells, *Nat. Phys.* **5**, 1 (2011).
- [33] L. Jiang, T. Kitagawa, J. Alicea, A. R. Akhmerov, D. Pekker, G. Refael, J. I. Cirac, E. Demler, M. D. Lukin, and P. Zoller, Majorana Fermions in Equilibrium and in Driven Cold-Atom Quantum Wires, *Phys. Rev. Lett.* **106**, 220402 (2011).
- [34] P. Hauke, O. Tieleman, A. Celi, C. Ölschläger, J. Simonet, J. Struck, M. Weinberg, P. Windpassinger, K. Sengstock, M. Lewenstein, and A. Eckardt, Non-Abelian Gauge Fields and Topological Insulators in Shaken Optical Lattices, *Phys. Rev. Lett.* **109**, 145301 (2012).
- [35] M. S. Rudner, N. H. Lindner, E. Berg, and M. Levin, Anomalous Edge States and the Bulk-Edge Correspondence for Periodically Driven Two-Dimensional Systems, *Phys. Rev. X* **3**, 031005 (2013).
- [36] N. Goldman and J. Dalibard, Periodically Driven Quantum Systems: Effective Hamiltonians and Engineered Gauge Fields, *Phys. Rev. X* **4**, 031027 (2014).
- [37] N. Goldman, J. Dalibard, M. Aidelsburger, and N. R. Cooper, Periodically driven quantum matter: The case of resonant modulations, *Phys. Rev. A* **91**, 033632 (2015).
- [38] A. C. Potter, T. Morimoto, and A. Vishwanath, Classification of Interacting Topological Floquet Phases in One Dimension, *Phys. Rev. X* **6**, 041001 (2016).
- [39] H. Chu, Po, L. Fidkowski, T. Morimoto, A. C. Potter, and A. Vishwanath, Chiral Floquet Phases of Many-Body Localized Bosons, *Phys. Rev. X* **6**, 041070 (2016).
- [40] A. Russomanno, A. Silva, and G. E. Santoro, Periodic Steady Regime and Interference in a Periodically Driven Quantum System, *Phys. Rev. Lett.* **109**, 257201 (2012).
- [41] L. D'Alessio and M. Rigol, Long-Time Behavior of Isolated Periodically Driven Interacting Lattice Systems, *Phys. Rev. X* **4**, 041048 (2014).
- [42] A. Lazarides, A. Das, and R. Moessner, Periodic Thermodynamics of Isolated Quantum Systems, *Phys. Rev. Lett.* **112**, 150401 (2014).
- [43] A. Chandran and S. L. Sondhi, Interaction-stabilized steady states in the driven  $O(N)$  model, *Phys. Rev. B* **93**, 174305 (2016).
- [44] R. Citro, Emanuele G. Dalla Torre, L. D'Alessio, A. Polkovnikov, M. Babadi, T. Oka, and E. Demler, Dynamical stability of a many-body Kapitza pendulum, *Ann. Phys.* **360**, 694 (2015).
- [45] P. Ponte, Z. Papić, F. Huvneers, and D. A. Abanin, Many-Body Localization in Periodically Driven Systems, *Phys. Rev. Lett.* **114**, 140401 (2015).
- [46] S. A. Weidinger and M. Knap, Floquet prethermalization and regimes of heating in a periodically driven, interacting quantum system, *Sci. Rep.* **7**, 45382 (2017).
- [47] Y. Hu, Z. Cai, M. A. Baranov, and P. Zoller, Majorana fermions in noisy Kitaev wires, *Phys. Rev. B* **92**, 165118 (2015).
- [48] P. Zoller, G. Alber, and R. Salvador, ac Stark splitting in intense stochastic driving fields with Gaussian statistics and non-Lorentzian line shape, *Phys. Rev. A* **24**, 398 (1981).
- [49] A. Mitra and T. Giamarchi, Mode-Coupling-Induced Dissipative and Thermal Effects at Long Times After a Quantum Quench, *Phys. Rev. Lett.* **107**, 150602 (2011).
- [50] A. Mitra and T. Giamarchi, Thermalization and dissipation in out-of-equilibrium quantum systems: A perturbative renormalization group approach, *Phys. Rev. B* **85**, 075117 (2012).
- [51] P. C. Hohenberg and B. I. Halperin, Theory of dynamic critical phenomena, *Rev. Mod. Phys.* **49**, 435 (1977).
- [52] A. Kamenev, *Field Theory of Non-Equilibrium Systems* (Cambridge University Press, Cambridge, 2011).
- [53] U. C. Taeuber, *Critical Dynamics: A Field Theory Approach to Equilibrium and Non-Equilibrium Scaling Behavior* (Cambridge University Press, Cambridge, 2014).
- [54] J. C. Phillips, Stretched exponential relaxation in molecular and electronic glasses, *Rep. Prog. Phys.* **59**, 1133 (1996).
- [55] R. V. Chamberlin, G. Mozurkewich, and R. Orbach, Time Decay of the Remanent Magnetization in Spin Glasses, *Phys. Rev. Lett.* **52**, 867 (1984).
- [56] D. Poletti, P. Barmettler, A. Georges, and C. Kollath, Emergence of Glasslike Dynamics for Dissipative and Strongly Interacting Bosons, *Phys. Rev. Lett.* **111**, 195301 (2013).
- [57] A. Carmele, M. Heyl, C. Kraus, and M. Dalmonte, Stretched exponential decay of Majorana edge modes in many-body localized Kitaev chains under dissipation, *Phys. Rev. B* **92**, 195107 (2015).
- [58] E. Levi, M. Heyl, I. Lesanovsky, and J. P. Garrahan, Robustness of Many-Body Localization in the Presence of Dissipation, *Phys. Rev. Lett.* **116**, 237203 (2016).
- [59] S. Gopalakrishnan, K. Ranjibul Islam, and M. Knap, Noise-induced Subdiffusion in Strongly Localized Quantum Systems, *Phys. Rev. Lett.* **119**, 046601 (2017).
- [60] M. H. Fischer, M. Maksymenko, and E. Altman, Dynamics of a Many-Body-Localized System Coupled to a Bath, *Phys. Rev. Lett.* **116**, 160401 (2016).
- [61] K. L. Ngai, Universality of low-frequency fluctuation, dissipation, and relaxation properties of condensed matter. I, *Comments Solid State Phys.* **9**, 127 (1979).
- [62] R. G. Palmer, D. L. Stein, E. Abrahams, and P. W. Anderson, Models of Hierarchically Constrained Dynamics for Glassy Relaxation, *Phys. Rev. Lett.* **53**, 958 (1984).
- [63] L. Berthier and G. Biroli, Theoretical perspective on the glass transition and amorphous materials, *Rev. Mod. Phys.* **83**, 587 (2011).
- [64] T. Giamarchi, *Quantum Physics in One Dimension* (Oxford University Press, Oxford, 2003).
- [65] H. P. Lüschen, P. Bordia, S. Scherg, F. Alet, E. Altman, U. Schneider, and I. Bloch, Evidence for Griffiths-type dynamics near the many-body localization transition in quasi-periodic systems, [arXiv:1612.07173](https://arxiv.org/abs/1612.07173).
- [66] M. Serbyn, Z. Papić, and D. A. Abanin, Quantum quenches in the many-body localized phase, *Phys. Rev. B* **90**, 174302 (2014).
- [67] K. Agarwal, S. Gopalakrishnan, M. Knap, M. Müller, and E. Demler, Anomalous Diffusion and Griffiths Effects Near the Many-Body Localization Transition, *Phys. Rev. Lett.* **114**, 160401 (2015).

- [68] P. Smacchia, M. Knap, E. Demler, and A. Silva, Exploring dynamical phase transitions and prethermalization with quantum noise of excitations, *Phys. Rev. B* **91**, 205136 (2015).
- [69] M. Moshe and J. Zinn-Justin, Quantum field theory in the large- $N$  limit: A review, *Phys. Rep.* **385**, 69 (2003).
- [70] S. Sachdev, *Quantum Phase Transitions* (Cambridge University Press, Cambridge, 1999).
- [71] M. Schreiber, S. S. Hodgman, P. Bordia, H. P. Lüschen, M. H. Fischer, R. Vosk, E. Altman, U. Schneider, and I. Bloch, Observation of many-body localization of interacting fermions in a quasirandom optical lattice, *Science* **349**, 842 (2015).
- [72] S. Nascimbène, Realizing one-dimensional topological superfluids with ultracold atomic gases, *J. Phys. B* **46**, 134005 (2013).
- [73] C. V. Kraus, S. Diehl, P. Zoller, and M. A. Baranov, Preparing and probing atomic Majorana fermions and topological order in optical lattices, *New J. Phys.* **14**, 113036 (2012).
- [74] Y. Hu and M. A. Baranov, Effects of gapless bosonic fluctuations on Majorana fermions in atomic wire coupled to a molecular reservoir, *Phys. Rev. A* **92**, 053615 (2015).
- [75] J. Billy, V. Josse, Z. Zuo, A. Bernard, B. Hambrecht, P. Lugan, D. Clement, L. Sanchez-Palencia, P. Bouyer, and A. Aspect, Direct observation of Anderson localization of matter waves in a controlled disorder, *Nature (London)* **453**, 891 (2008).
- [76] S. Baier, M. J. Mark, D. Petter, K. Aikawa, L. Chomaz, Z. Cai, M. Baranov, P. Zoller, and F. Ferlaino, Extended Bose-Hubbard models with ultracold magnetic atoms, *Science* **352**, 201 (2016).
- [77] A. L. Gaunt, T. F. Schmidutz, I. Gotlibovych, R. P. Smith, and Z. Hadzibabic, Bose-Einstein Condensation of Atoms in a Uniform Potential, *Phys. Rev. Lett.* **110**, 200406 (2013).
- [78] U. Schollwöck, The density-matrix renormalization group, *Rev. Mod. Phys.* **77**, 259 (2005).
- [79] A. J. Daley, C. Kollath, U. Schollwöck, and G. Vidal, Time-dependent density-matrix renormalization-group using adaptive effective Hilbert spaces, *J. Stat. Mech* (2004) P04005.
- [80] M. Hartmann, D. Poletti, M. Ivanchenko, S. Denisov, and P. Hänggi, Asymptotic state of many-body open quantum systems: A role of interaction, [arXiv:1606.03896](https://arxiv.org/abs/1606.03896).
- [81] M. Heyl, A. Polkovnikov, and S. Kehrein, Dynamical Quantum Phase Transitions in the Transverse-Field Ising Model, *Phys. Rev. Lett.* **110**, 135704 (2013).
- [82] M. Heyl, Scaling and Universality at Dynamical Quantum Phase Transitions, *Phys. Rev. Lett.* **115**, 140602 (2015).
- [83] J. M. Zhang and H.-T. Yang, Cusps in the quench dynamics of a Bloch state, *Europhys. Lett.* **114**, 60001 (2016).